IPI Letters

ISSN 2976 - 730X
IPI Letters 2026,Vol 4 (2):21-40
https://doi.org/10.59973/ipil.354

Received: 2026-04-16
Accepted: 2026-04-18
Published: 2026-04-22

Article

A Regularized Variational Framework for Metric-Type Geometry from Discrete Anchors

Raoul Bianchetti[1,*], **Payam Danesh**[2]

[1] Information Physics Institute, Gosport, Hampshire, United Kingdom, www.informationphysicsinstitute.org
[2] Department of Biosystems Engineering, Faculty of Agricultural Science, University of Tehran, Tehran, Iran

[*]Corresponding author: raoul.bianchetti@informationphysicsinstitute.net

Abstract - We formulate and analyze a regularized variational model in which finitely many discrete anchors constrain a scalar field on a bounded Lipschitz domain and, through second-order response, determine a tensorial object of metric type. The analytic point of departure is that singular pointwise anchoring is incompatible with the natural Sobolev setting of the Dirichlet energy. To overcome this difficulty, each anchor is represented by a mollified averaging functional, so that the full anchor mechanism becomes continuous on the admissible class and remains compatible with weak convergence. The resulting action consists of a Dirichlet term, a weighted anchor-fidelity term, and an auxiliary regularization term. Within this framework we derive the first variation, the weak Euler–Lagrange equation, and the second variation in complete form. We then prove existence of minimizers under standard coercivity and weak lower-semicontinuity hypotheses, establish uniqueness under strict convexity, and show that the second-order response is symmetric and positive semidefinite when the regularization is convex. In the quadratic regularization case we obtain a linear elliptic field equation with smooth localized forcing and record the corresponding interior regularity consequences. The geometric conclusion of the paper is stated at its natural level of generality: whenever the second-order response admits a local tensor representation and satisfies an explicit nondegeneracy condition relative to a positive definite reference tensor, it induces a continuous metric-type tensor on the region under consideration. A finite-difference discretization of the quadratic model is also constructed, validated by a manufactured-solution experiment, and used to study the dependence of the reconstructed response tensor on the anchor-fidelity and anchor-width parameters. The paper therefore provides a mathematically controlled Euclidean variational framework in which localized discrete data determine a field and, under explicit hypotheses, a geometric response of metric type.

Keywords - Calculus of variations; Sobolev spaces; Elliptic variational problems; Regularized anchor constraints; Metric-type tensors; Finite differences.

1 Introduction

In the standard mathematical treatment of geometry and field theory, the geometric tensor is prescribed at the beginning of the analysis. One starts with a manifold endowed with a metric or metric-like structure and then studies operators, variational principles, and differential equations relative to that background [1]. The present paper addresses a more preliminary question. Suppose that one is given only a scalar variational field together with finitely many localized data constraints. Can the second-order response of the resulting variational problem produce an object that is legitimately geometric in character, at least in the limited sense of a continuous symmetric tensor of metric

type? At the level of general motivation, this question is adjacent to information geometry [2]. It is also adjacent, in a much broader conceptual sense, to proposals in which geometric connectedness is related to quantum entanglement [3]. A closely related reference in that direction is the holographic perspective developed by Swingle [4]. The aim of the present manuscript, however, is not to merge those theories or to restate their claims in different language. It is to isolate one concrete variational model and to determine, with full analytic precision, what that model does and does not prove.

That restriction of scope is deliberate. Expressions such as *emergent geometry* or *information-induced geometry* can become broader than the analytic mechanisms meant to support them. A mathematics paper must proceed in the opposite direction. One first specifies the admissible class, then the action functional, then the corresponding first- and second-order variational formulas, and only after that asks what geometric interpretation, if any, survives mathematical scrutiny. Geometry is therefore not inserted as hidden input and later relabeled as emergent. It enters, if it enters at all, only through the second-order response of a rigorously defined anchored action.

The model is posed on a bounded Euclidean domain and therefore begins from a fixed analytic stage rather than from a background-free ontology. Concretely, we fix a bounded domain $\Omega \subset \mathbb{R}^d$, a finite family of discrete anchors

$$\mathcal{A} = \{(a_i, s_i)\}_{i=1}^{N} \subset \Omega \times \mathbb{R}, \tag{1}$$

and a scalar field

$$\Phi : \Omega \to \mathbb{R}. \tag{2}$$

The anchor location a_i records where the i-th datum acts, while the scalar s_i records the prescribed value associated with that location. No tensor field is assumed among the primitive data. The mathematical problem is to understand how the finite anchor family influences the minimizing field and whether the second-order response of the resulting variational problem can be organized into a tensorial object.

The Sobolev framework used here is classical, but several modern characterizations of Sobolev regularity and related limit formulas have recently been revisited in a unified way by Brezis, Seeger, Van Schaftingen, and Yung [5]. The continuity properties of classical Sobolev spaces and the failure of pointwise evaluation at low regularity are treated systematically in Adams and Fournier [6]. A broad account of fractional Sobolev spaces and nonlocal seminorms is given by Leoni [7]. These references clarify why singular anchoring is analytically unstable in the natural H^1-setting and why the present model must replace point constraints by regularized local averages.

The first analytic obstruction is therefore immediate. If the admissible class is chosen in the natural Sobolev space $H^1(\Omega)$, then point evaluation is generally not a continuous linear functional when $d \geq 2$. Consequently, a literal anchoring rule of the form $\Phi(a_i) = s_i$ is not suitable as the foundational ingredient of a direct-method variational theory. The remedy adopted here is to replace singular point constraints by regularized anchor operators obtained from mollified local averages. This places each anchor in the form of a bounded linear functional and restores compatibility with weak compactness, lower semicontinuity, and elliptic variational structure.

The direct-method foundation for the variational argument belongs to the classical framework developed by Dacorogna [8]. A complementary convex-analytic viewpoint is provided by Ekeland and Temam [9]. Standard properties of mollifiers and weak formulations for second-order equations are treated in Evans [10]. Interior regularity for the quadratic model is governed by the classical elliptic theory of Gilbarg and Trudinger [11]. Boundary regularity on nonsmooth domains is treated in the monograph of Grisvard [12]. The consistency and convergence diagnostics for the finite-difference discretization are drawn from the standard finite-difference framework presented by Strikwerda [13].

With these analytical tools in place, the main contributions of the paper can be stated precisely. First, the anchored action is formulated in a Sobolev-compatible manner through mollified anchor operators. Second, the first and second variations are computed explicitly, with every term written in a form suitable for weak analysis. Third, the direct method yields existence of minimizers under standard hypotheses, and strict convexity yields uniqueness in the quadratic case. Fourth, the second variation is shown to be symmetric and, under convexity of the auxiliary regularization, positive semidefinite. Fifth, a conditional metric-inducibility theorem is established: if the second-order response admits a local tensor representation and satisfies a nondegeneracy condition relative to a positive definite reference tensor, then it defines a continuous metric-type tensor on the region under

consideration. Finally, the quadratic model admits a finite-difference approximation whose accuracy is validated by mesh-refinement diagnostics and whose second-order response can be explored under systematic parameter variation.

It is equally important to state what the paper does *not* prove. The reference setting is Euclidean, the governing operator is elliptic, and the induced tensor is asserted only under explicit locality and nondegeneracy hypotheses. No Lorentzian signature is derived. No causal structure is obtained. No claim is made that physical spacetime has been reconstructed in full. The scope of the manuscript is narrower and, for that reason, mathematically firmer: it supplies a clean variational mechanism by which finitely many discrete localized data determine a scalar field and, under explicit second-order assumptions, a tensorial object of metric type.

The paper is organized as follows. Section 2 fixes the functional setting, the notation, the regularized anchor operators, and the anchored action. Section 3 derives the first and second variations and records the operator structure of the quadratic model. Section 4 contains the principal analytical statements, including existence, uniqueness under strict convexity, stationarity, elliptic regularity, and the metric-inducibility theorem. Section 5 develops the finite-difference discretization, validates it by a manufactured-solution experiment, and presents the anchor-driven numerical illustrations. Section 6 explains the exact mathematical scope of the framework, and the appendix supplies expanded proofs and supporting estimates.

2 Functional framework and regularized anchored action

This section fixes the analytic setting once and for all. The presentation is intentionally slower than the introductory summary, because every later theorem depends on the precise meaning of the admissible class, the anchor operators, and the action functional. The governing philosophy is simple: the model should be stated in a Sobolev framework strong enough to support elliptic variational analysis, but flexible enough to encode the discrete anchor data without introducing singular constraints.

2.1 Domain, anchors, and admissible class

Let $\Omega \subset \mathbb{R}^d$ be a bounded open set with Lipschitz boundary. This hypothesis is used repeatedly and is part of the standing analytical framework of the model. It ensures the Sobolev trace theorem, the compact embedding of $H^1(\Omega)$ into $L^2(\Omega)$, and the weak sequential compactness properties needed later in the direct-method argument. The discrete input of the model is a finite family of anchors

$$\mathcal{A} = \{(a_i, s_i)\}_{i=1}^{N}, \qquad a_i \in \Omega, \qquad s_i \in \mathbb{R}. \tag{3}$$

The quantity a_i records the spatial location of the i-th anchor and s_i the corresponding scalar datum.

The unknown is a scalar field Φ. At this stage there is no tensorial object in the formulation; the problem begins with a single scalar variational unknown. Unless otherwise stated, we work with the admissible class

$$\mathcal{V} = H_0^1(\Omega). \tag{4}$$

Nothing essential changes if one replaces $H_0^1(\Omega)$ by a closed convex affine subspace of $H^1(\Omega)$ corresponding to prescribed Dirichlet boundary data. The homogeneous case is adopted for clarity, because it keeps the notation lean and removes the additive-constant null direction that would otherwise remain in the pure Dirichlet term. In particular, the quadratic model acquires a transparent coercive structure on $H_0^1(\Omega)$.

For ease of reference, the principal symbols used throughout the paper are collected in Table 1. The same notation reappears in the direct-method argument, in the second-variation formulas, and again in the discrete approximation. Fixing it here prevents a shift in meaning later in the manuscript, especially for the response tensor and the discrete tensor proxy, which must remain conceptually distinct.

Table 1: Principal notation used throughout the manuscript.

Symbol	Meaning
Ω	bounded reference domain in $\mathbb{R}^d$ with Lipschitz boundary
$\mathcal{A} = \{(a_i, s_i)\}_{i=1}^N$	finite discrete anchor family
$\mathcal{V}$	admissible class, usually $H_0^1(\Omega)$
Φ	coherence field, i.e. the scalar variational unknown
ρ_ε	mollified kernel at scale ε
$\ell_{i,\varepsilon}$	regularized anchor functional associated with a_i
λ	anchor-fidelity parameter
μ	auxiliary regularization parameter
$\mathcal{R}$	additional regularization functional
$\mathcal{J}$	regularized anchored action
$\delta\mathcal{J}$, $\delta^2\mathcal{J}$	first and second variations of the action
Φ_*	a minimizer of $\mathcal{J}$
$\mathcal{T}$	local coherence-response tensor, when representability holds
g	derived metric-type tensor induced from $\mathcal{T}$
Φ_h	discrete field approximation on the numerical grid
H_h	discrete Hessian of the computed field
T_h	positive-semidefinite tensor proxy reconstructed from H_h

2.2 Regularized anchors

The anchor mechanism is introduced through mollified local averages. This is the point at which the discrete data enter the continuum model, and it is also the point at which the variational framework must be handled most carefully. Let $\rho \in C_c^\infty(\mathbb{R}^d)$ satisfy

$$\rho \geq 0, \qquad \int_{\mathbb{R}^d} \rho(x)\, \mathrm{d}x = 1. \tag{5}$$

For $\varepsilon > 0$ define the rescaled family

$$\rho_\varepsilon(x) = \varepsilon^{-d} \rho(x/\varepsilon). \tag{6}$$

If $a_i \in \Omega$, the corresponding regularized anchor functional is

$$\ell_{i,\varepsilon}(\Phi) = \int_\Omega \rho_\varepsilon(x - a_i)\, \Phi(x)\, \mathrm{d}x. \tag{7}$$

The support of $\rho_\varepsilon(\cdot - a_i)$ determines the effective coherence region through which the anchor acts.

The mathematical role of the regularization scale is displayed in Figure 1. The parameter ε does not merely smooth the graph visually; it changes the anchor operator itself by changing the averaging radius in (7). When ε is small, the anchor functional is sharply localized and the model approaches a concentrated probing regime. When ε is larger, the same datum acts through a broader neighborhood, which weakens peak curvature and distributes the response more evenly in space.

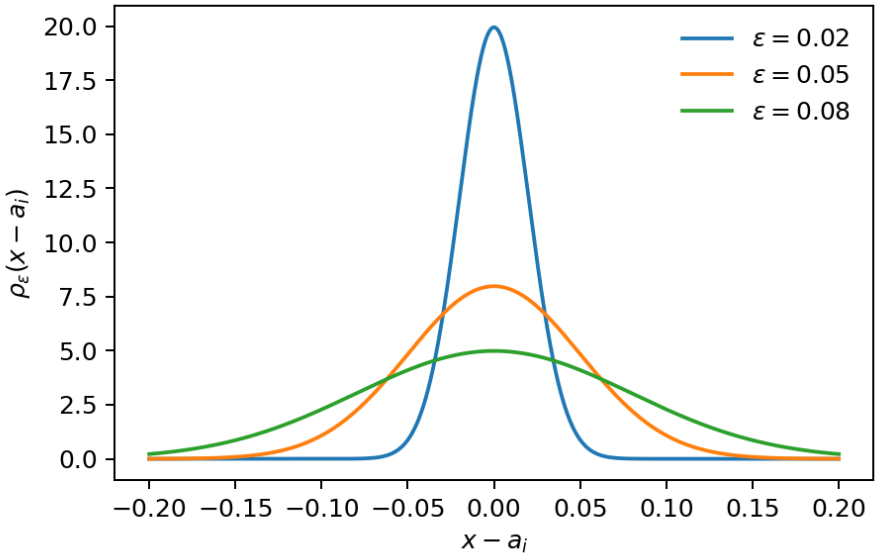

Figure 1: One-dimensional sections of the regularized kernel $\rho_\varepsilon(x - a_i)$ for three values of ε. Smaller ε produces a sharply localized anchor; larger ε spreads the same anchor information over a wider neighborhood.

The regularized formulation is the key analytic correction that makes the model rigorous. It converts each anchor into a bounded linear functional on the admissible space and thereby makes the anchor-fidelity term compatible with weak convergence.

Proposition 2.1. *For each i and $\varepsilon > 0$, the map $\ell_{i,\varepsilon} : H^1(\Omega) \to \mathbb{R}$ is linear and continuous.*

Proof. Linearity is immediate from (7). Since $\rho_\varepsilon(\cdot - a_i) \in L^2(\Omega)$, the Cauchy–Schwarz inequality yields

$$|\ell_{i,\varepsilon}(\Phi)| \le \left\|\rho_\varepsilon(\cdot - a_i)\right\|_{L^2(\Omega)} \|\Phi\|_{L^2(\Omega)}. \tag{8}$$

The continuous embedding $H^1(\Omega) \hookrightarrow L^2(\Omega)$ then gives

$$|\ell_{i,\varepsilon}(\Phi)| \le C_{\Omega,\varepsilon,i} \|\Phi\|_{H^1(\Omega)}. \tag{9}$$

Hence $\ell_{i,\varepsilon}$ is continuous. □

2.3 The anchored action

We now define the energy functional that governs the model.

Definition 2.2. Let $w_i > 0$, $\lambda > 0$, and $\mu \ge 0$. Let $\mathcal{R} : \mathcal{V} \to \mathbb{R} \cup \{+\infty\}$ be weakly lower semicontinuous. The regularized anchored action is

$$\mathcal{J}(\Phi) = \frac{1}{2}\int_\Omega |\nabla\Phi|^2 \, dx + \frac{\lambda}{2}\sum_{i=1}^{N} w_i\Big(\ell_{i,\varepsilon}(\Phi) - s_i\Big)^2 + \mu\,\mathcal{R}(\Phi), \qquad \Phi \in \mathcal{V}. \tag{10}$$

The first point to note is that $\mathcal{J}$ is not a purely formal expression.

Proposition 2.3. *Assume that $\mathcal{R}$ is finite on $\mathcal{V}$. Then the functional $\mathcal{J} : \mathcal{V} \to \mathbb{R}$ given by* (10) *is well defined. Moreover, the anchor-fidelity term*

$$\Phi \longmapsto \frac{\lambda}{2}\sum_{i=1}^{N} w_i\Big(\ell_{i,\varepsilon}(\Phi) - s_i\Big)^2 \tag{11}$$

is weakly continuous on $\mathcal{V}$.

Proof. The Dirichlet term is finite for every $\Phi \in H^1_0(\Omega)$, and the regularization term is finite by assumption. By Proposition 2.1, each map $\ell_{i,\varepsilon}$ is continuous on $H^1(\Omega)$, hence on $\mathcal{V}$. Therefore every summand in (11) is finite and continuous, so $\mathcal{J}$ is well defined. If $\Phi_n \rightharpoonup \Phi$ weakly in $\mathcal{V}$, then continuity of the linear functionals $\ell_{i,\varepsilon}$ gives $\ell_{i,\varepsilon}(\Phi_n) \to \ell_{i,\varepsilon}(\Phi)$ for each i. Because the anchor family is finite, the sum of squares converges as well, which proves weak continuity of the anchor term. □

Each term has a distinct purpose. The Dirichlet energy controls oscillation and provides the elliptic core of the problem. The anchor-fidelity term couples the continuum field to the finite anchor data. The auxiliary regularization $\mathcal{R}$ may be used to strengthen coercivity or to impose additional structure. The case of greatest interest in both the analysis and the numerics is the quadratic choice

$$\mathcal{R}(\Phi) = \frac{1}{2}\int_\Omega |\Phi|^2 \, \mathrm{d}x, \tag{12}$$

for which the action becomes

$$\mathcal{J}(\Phi) = \frac{1}{2}\int_\Omega |\nabla\Phi|^2 \, \mathrm{d}x + \frac{\lambda}{2}\sum_{i=1}^{N} w_i\Big(\ell_{i,\varepsilon}(\Phi) - s_i\Big)^2 + \frac{\mu}{2}\int_\Omega |\Phi|^2 \, \mathrm{d}x. \tag{13}$$

The structure of (10) is partly local and partly nonlocal. The gradient term and the quadratic regularization are local; the anchor term is nonlocal because each $\ell_{i,\varepsilon}$ averages Φ over a neighborhood of a_i. This combination is exactly what the model requires: a field theory with local elliptic regularity, constrained by finitely many localized but nonsingular data channels.

2.4 Standing hypotheses for the analytical sections

Theorems in the remainder of the paper will invoke additional hypotheses only when they are genuinely needed. Nevertheless, it is useful to record the standing conventions in one place.

Assumption 2.4. Unless explicitly stated otherwise, $\Omega \subset \mathbb{R}^d$ is bounded with Lipschitz boundary and the admissible class $\mathcal{V}$ is a nonempty closed convex subset of $H^1(\Omega)$; in the model case, $\mathcal{V} = H^1_0(\Omega)$.

Assumption 2.5. For existence statements, $\mathcal{R}$ is assumed weakly lower semicontinuous on $\mathcal{V}$. For first-variation statements, $\mathcal{R}$ is assumed Gâteaux differentiable on $\mathcal{V}$. For second-variation statements, $\mathcal{R}$ is assumed twice Gâteaux differentiable on $\mathcal{V}$.

Assumption 2.6. Whenever positivity of the second variation is asserted, the regularization $\mathcal{R}$ is additionally assumed convex.

These assumptions are intentionally modest. None of them presupposes the existence of a geometric tensor. Their role is to ensure that the variational problem is well posed and that the passage from first-order stationarity to second-order response can be justified without hidden regularity assumptions.

3 First and second variation

With the functional framework in place, the next task is to compute the first and second derivatives of the action in a form suitable for analysis. The formulas in this section are elementary in principle, but they carry the full structural content of the model. The first variation identifies the field equation satisfied by minimizers, while the second variation identifies the response form from which the later geometric interpretation is extracted.

The logical order is important. One does not begin by declaring a tensor and then searching for a variational expression that reproduces it. One begins with the anchored action, differentiates it carefully, and studies the resulting bilinear response on the admissible perturbation space. Only after those steps have been completed does any tensorial language become legitimate. That discipline is what keeps the present paper within the standards of a rigorous analysis article.

3.1 First variation and weak Euler–Lagrange equation

Assume from now on that $\mathcal{R}$ is Gâteaux differentiable on $\mathcal{V}$. Fix $\Phi, \psi \in \mathcal{V}$ and consider the scalar function

$$F(t) = \mathcal{J}(\Phi + t\psi), \qquad t \in \mathbb{R} \tag{14}$$

for all t small enough that $\Phi + t\psi \in \mathcal{V}$. The first variation of $\mathcal{J}$ at Φ in the direction ψ is, by definition,

$$\delta\mathcal{J}(\Phi)[\psi] = F'(0). \tag{15}$$

Because the action is the sum of three terms, it is natural to differentiate each term separately.

For the Dirichlet contribution one has

$$\frac{\mathrm{d}}{\mathrm{d}t}\Big|_{t=0}\frac{1}{2}\int_\Omega |\nabla(\Phi+t\psi)|^2\,\mathrm{d}x = \int_\Omega \nabla\Phi\cdot\nabla\psi\,\mathrm{d}x. \tag{16}$$

For the anchor-fidelity term, linearity of $\ell_{i,\varepsilon}$ gives

$$\ell_{i,\varepsilon}(\Phi+t\psi) = \ell_{i,\varepsilon}(\Phi) + t\,\ell_{i,\varepsilon}(\psi), \tag{17}$$

and therefore

$$\frac{\mathrm{d}}{\mathrm{d}t}\Big|_{t=0}\frac{\lambda}{2}\sum_{i=1}^N w_i\Big(\ell_{i,\varepsilon}(\Phi+t\psi)-s_i\Big)^2 = \lambda\sum_{i=1}^N w_i\Big(\ell_{i,\varepsilon}(\Phi)-s_i\Big)\ell_{i,\varepsilon}(\psi). \tag{18}$$

Finally, differentiability of $\mathcal{R}$ yields

$$\frac{\mathrm{d}}{\mathrm{d}t}\Big|_{t=0}\mu\,\mathcal{R}(\Phi+t\psi) = \mu\,\delta\mathcal{R}(\Phi)[\psi]. \tag{19}$$

Combining (16)–(19), one obtains the first variation formula

$$\delta\mathcal{J}(\Phi)[\psi] = \int_\Omega \nabla\Phi\cdot\nabla\psi\,\mathrm{d}x + \lambda\sum_{i=1}^N w_i\Big(\ell_{i,\varepsilon}(\Phi)-s_i\Big)\,\ell_{i,\varepsilon}(\psi) + \mu\,\delta\mathcal{R}(\Phi)[\psi]. \tag{20}$$

Formula (20) already displays the architecture of the model. The first term is local and elliptic, the second is finite-rank and nonlocal through the anchor averages, and the third records whatever additional structure is imposed by the regularization. A minimizer $\Phi_*\in\mathcal{V}$ must satisfy

$$\delta\mathcal{J}(\Phi_*)[\psi] = 0 \qquad \text{for all } \psi\in\mathcal{V}, \tag{21}$$

and hence is characterized by the weak identity

$$\int_\Omega \nabla\Phi_*\cdot\nabla\psi\,\mathrm{d}x + \lambda\sum_{i=1}^N w_i\Big(\ell_{i,\varepsilon}(\Phi_*)-s_i\Big)\,\ell_{i,\varepsilon}(\psi) + \mu\,\delta\mathcal{R}(\Phi_*)[\psi] = 0 \tag{22}$$

for every $\psi\in\mathcal{V}$.

In the quadratic case (12), the last term becomes explicit and the weak equation takes the form

$$\int_\Omega \nabla\Phi_*\cdot\nabla\psi\,\mathrm{d}x + \lambda\sum_{i=1}^N w_i\Big(\ell_{i,\varepsilon}(\Phi_*)-s_i\Big)\,\ell_{i,\varepsilon}(\psi) + \mu\int_\Omega \Phi_*\psi\,\mathrm{d}x = 0. \tag{23}$$

If Φ_* is regular enough to justify integration by parts, then (23) can be rewritten in strong form as

$$-\Delta\Phi_* + \mu\,\Phi_* + \lambda\sum_{i=1}^N w_i\Big(\ell_{i,\varepsilon}(\Phi_*)-s_i\Big)\rho_\varepsilon(\cdot-a_i) = 0 \quad \text{in } \Omega, \qquad \Phi_* = 0 \quad \text{on } \partial\Omega. \tag{24}$$

Equation (24) shows why the regularized model is analytically tractable: the anchors appear as smooth localized forcing profiles rather than as singular point sources.

3.2 Second variation and response form

Assume now that $\mathcal{R}$ is twice Gâteaux differentiable. Fix $\Phi\in\mathcal{V}$ and $\psi,\eta\in\mathcal{V}$. The second variation is obtained by differentiating the first variation with respect to the base point:

$$\delta^2\mathcal{J}(\Phi)[\psi,\eta] = \frac{\mathrm{d}}{\mathrm{d}t}\Big|_{t=0}\delta\mathcal{J}(\Phi+t\eta)[\psi]. \tag{25}$$

As before, the three pieces of the action can be differentiated separately. The Dirichlet term gives

$$\frac{\mathrm{d}}{\mathrm{d}t}\Big|_{t=0}\int_\Omega \nabla(\Phi+t\eta)\cdot\nabla\psi\,\mathrm{d}x = \int_\Omega \nabla\eta\cdot\nabla\psi\,\mathrm{d}x. \tag{26}$$

For the anchor term, (17) yields

$$\frac{\mathrm{d}}{\mathrm{d}t}\Big|_{t=0}\lambda\sum_{i=1}^{N} w_i\Big(\ell_{i,\varepsilon}(\Phi+t\eta)-s_i\Big)\ell_{i,\varepsilon}(\psi)=\lambda\sum_{i=1}^{N} w_i\,\ell_{i,\varepsilon}(\eta)\,\ell_{i,\varepsilon}(\psi). \tag{27}$$

Finally,

$$\frac{\mathrm{d}}{\mathrm{d}t}\Big|_{t=0}\mu\,\delta\mathcal{R}(\Phi+t\eta)[\psi]=\mu\,\delta^2\mathcal{R}(\Phi)[\psi,\eta]. \tag{28}$$

Therefore

$$\delta^2\mathcal{J}(\Phi)[\psi,\eta]=\int_\Omega \nabla\psi\cdot\nabla\eta\;\mathrm{d}x+\lambda\sum_{i=1}^{N} w_i\,\ell_{i,\varepsilon}(\psi)\,\ell_{i,\varepsilon}(\eta)+\mu\,\delta^2\mathcal{R}(\Phi)[\psi,\eta]. \tag{29}$$

The form (29) is the central second-order object of the theory. It is a bilinear response form on perturbations, not yet a pointwise tensor field. This distinction matters. The variational analysis proves the existence of the bilinear form directly. Any pointwise tensorial object must later be obtained, if at all, by an additional representability argument.

In the quadratic case (12), the dependence on the base point Φ disappears from the regularization term and one obtains the especially transparent formula

$$\delta^2\mathcal{J}(\Phi)[\psi,\eta]=\int_\Omega \nabla\psi\cdot\nabla\eta\;\mathrm{d}x+\lambda\sum_{i=1}^{N} w_i\,\ell_{i,\varepsilon}(\psi)\,\ell_{i,\varepsilon}(\eta)+\mu\int_\Omega \psi\eta\;\mathrm{d}x. \tag{30}$$

Two structural consequences are immediate and fundamental.

Proposition 3.1. *Assume that $\mathcal{R}$ is convex and twice Gâteaux differentiable. Then for every $\Phi\in\mathcal{V}$ the bilinear form $\delta^2\mathcal{J}(\Phi)$ is symmetric and positive semidefinite:*

$$\delta^2\mathcal{J}(\Phi)[\psi,\eta]=\delta^2\mathcal{J}(\Phi)[\eta,\psi], \tag{31}$$

and

$$\delta^2\mathcal{J}(\Phi)[\psi,\psi]\geq 0\qquad \text{for all } \psi\in\mathcal{V}. \tag{32}$$

Proof. Symmetry follows term by term from (29): the gradient pairing is symmetric, the product $\ell_{i,\varepsilon}(\psi)\ell_{i,\varepsilon}(\eta)$ is symmetric in ψ and η, and the second differential of a scalar functional is symmetric under the present differentiability hypotheses. To prove positivity, set $\eta=\psi$ in (29) and obtain

$$\delta^2\mathcal{J}(\Phi)[\psi,\psi]=\int_\Omega |\nabla\psi|^2\;\mathrm{d}x+\lambda\sum_{i=1}^{N} w_i\Big(\ell_{i,\varepsilon}(\psi)\Big)^2+\mu\,\delta^2\mathcal{R}(\Phi)[\psi,\psi]. \tag{33}$$

The first two terms are manifestly nonnegative. The last term is nonnegative because convexity of $\mathcal{R}$ implies positivity of its second variation. Hence (32) follows. □

3.3 Operator form

In the quadratic case the response form is represented by the operator

$$L_{\varepsilon,\lambda,\mu}\psi=-\Delta\psi+\mu\,\psi+\lambda\sum_{i=1}^{N} w_i\,\ell_{i,\varepsilon}(\psi)\,\rho_\varepsilon(\cdot-a_i), \tag{34}$$

in the sense that

$$\delta^2\mathcal{J}(\Phi)[\psi,\eta]=\int_\Omega (L_{\varepsilon,\lambda,\mu}\psi)\,\eta\;\mathrm{d}x \tag{35}$$

for smooth test functions ψ,η satisfying the boundary conditions. The principal symbol of $L_{\varepsilon,\lambda,\mu}$ is

$$\sigma_{\mathrm{prin}}(L_{\varepsilon,\lambda,\mu})(x,\xi)=|\xi|^2. \tag{36}$$

Hence the model remains elliptic at leading order; the anchor term is a finite-rank nonlocal perturbation of a uniformly elliptic operator. This point will matter later when we interpret the induced tensorial structure: the response is fundamentally an elliptic response.

4 Main analytical results

The purpose of this section is to convert the structural formulas of Section 3 into theorem-level statements. The order of presentation is deliberate. We begin with existence, because no response analysis is meaningful until the variational problem is known to possess at least one minimizing configuration. We then address uniqueness under strict convexity, stationarity of minimizers, elliptic regularity in the quadratic case, and finally the conditional passage from the second-order response form to a metric-type tensor.

4.1 Existence of minimizers

The first foundational issue is whether the action $\mathcal{J}$ actually selects a field configuration in the admissible class.

Assumption 4.1. The functional $\mathcal{J}$ is coercive on $\mathcal{V}$, that is,

$$\|\Phi\|_{H^1(\Omega)} \to \infty \quad \Longrightarrow \quad \mathcal{J}(\Phi) \to +\infty. \tag{37}$$

Theorem 4.2. *Assume that $\mathcal{V} \subset H^1(\Omega)$ is nonempty, closed, and convex, that $\mathcal{R}$ is weakly lower semicontinuous on $\mathcal{V}$, and that $\mathcal{J}$ is coercive. Then there exists at least one minimizer $\Phi_* \in \mathcal{V}$ such that*

$$\mathcal{J}(\Phi_*) = \inf_{\Phi \in \mathcal{V}} \mathcal{J}(\Phi). \tag{38}$$

Proof. The proof is a standard direct-method argument in the calculus of variations. A complementary convex-analytic perspective is developed in. For completeness, a detailed proof is given in Appendix A.2. □

Theorem 4.2 is the minimal well-posedness statement required for the rest of the paper. It guarantees that the anchored action selects at least one variational state in the admissible class, rather than merely defining a formal optimization problem.

Proposition 4.3. *Assume the hypotheses of Theorem 4.2. If, in addition, $\mathcal{J}$ is strictly convex on $\mathcal{V}$, then the minimizer is unique.*

Proof. Suppose that $\Phi_1, \Phi_2 \in \mathcal{V}$ are distinct minimizers. For $0 < t < 1$, convexity of $\mathcal{V}$ implies $t\Phi_1 + (1-t)\Phi_2 \in \mathcal{V}$. Strict convexity of $\mathcal{J}$ then yields

$$\mathcal{J}(t\Phi_1 + (1-t)\Phi_2) < t\mathcal{J}(\Phi_1) + (1-t)\mathcal{J}(\Phi_2), \tag{39}$$

which is impossible because the right-hand side equals the minimal value of $\mathcal{J}$. Hence $\Phi_1 = \Phi_2$. □

In the quadratic case (13) with $\mathcal{V} = H^1_0(\Omega)$, coercivity is immediate from Poincaré's inequality:

$$\mathcal{J}(\Phi) \geq \frac{1}{2}\|\nabla\Phi\|^2_{L^2(\Omega)} + \frac{\mu}{2}\|\Phi\|^2_{L^2(\Omega)} - \frac{\lambda}{2}\sum_{i=1}^{N} w_i s_i^2, \tag{40}$$

so the admissible sequence cannot escape to infinity in $H^1_0(\Omega)$.

4.2 Stationarity and regularity

Once existence is established, the minimizer must be linked back to the variational equations derived earlier. This step is conceptually important. The direct method provides existence in the admissible class, but the Euler–Lagrange theory identifies the equation actually solved by the minimizing field. In the present model, the two viewpoints coincide in the usual way.

Proposition 4.4. *Let Φ_* be a minimizer of $\mathcal{J}$, and assume that $\mathcal{R}$ is Gâteaux differentiable. Then Φ_* satisfies* (22).

Proof. For every $\psi \in \mathcal{V}$, the scalar function $t \mapsto \mathcal{J}(\Phi_* + t\psi)$ has a minimum at $t = 0$. Differentiating at $t = 0$ yields $\delta\mathcal{J}(\Phi_*)[\psi] = 0$. □

The quadratic case admits additional regularity because the strong equation (24) is a linear elliptic equation with smooth forcing profiles. The regularity statement below should be read as a theorem about the *regularized* anchor model. It is the mollified forcing, together with ellipticity, that makes the improved regularity available.

Proposition 4.5. *Assume the quadratic regularization* (12). *Let* $\Phi_* \in H^1_0(\Omega)$ *be a minimizer. Then* Φ_* *is a weak solution of* (24). *Moreover,*

$$\Phi_* \in H^2_{\mathrm{loc}}(\Omega). \tag{41}$$

If $\partial\Omega$ *is of class* $C^{1,1}$, *then* $\Phi_* \in H^2(\Omega)$. *If* $\rho \in C^\infty_c(\mathbb{R}^d)$, *then* Φ_* *is smooth in the interior of* Ω.

Proof. The forcing term in (24) is a finite linear combination of smooth compactly supported kernels. The stated interior regularity follows from standard elliptic theory. For boundary regularity issues on nonsmooth domains, see the classical treatment in Grisvard. □

4.3 Conditional tensor representation and metric inducibility

The geometric step is the most delicate one in the paper, because a bilinear form on perturbations does not by itself produce a tensor field pointwise on Ω. A local tensor representation must therefore be imposed as an additional hypothesis rather than inferred automatically from notation alone. In particular, the present argument never identifies the scalar field Φ_* itself with geometry. The field remains a variational unknown on the reference domain. What carries geometric content is the second-order response of the action at Φ_*, and even then only on those regions where representability and nondegeneracy can be justified.

The passage from response form to tensor field is the most delicate point in the paper. The second variation is a bilinear form on admissible perturbations. It is therefore a global variational object. A pointwise tensor field, by contrast, is a local geometric object. One cannot pass from the first to the second merely by notation. A separate local representability hypothesis is required, and the theorem below is written so that this point is explicit rather than hidden.

Definition 4.6. Let $U \subset \Omega$ be open, and let Φ_* be a minimizer. We say that the second-order response admits a local tensor representation on U if there exists a continuous symmetric $(0,2)$-tensor field $\mathcal{T}$ on U such that the local response density can be represented by $\mathcal{T}$ in the model under consideration. In that case $\mathcal{T}$ is called the *coherence-response tensor*.

The purpose of Definition 4.6 is not to hide a proof gap; it is to state honestly where the variational theorem stops and where an additional representability assumption begins. The bilinear form (29) is proved. A pointwise tensor field requires more.

Theorem 4.7. *Let* $U \subset \Omega$ *be open. Assume that*

(i) Φ_* *is a minimizer of* $\mathcal{J}$;

(ii) the second variation is symmetric and positive semidefinite;

(iii) the second-order response admits on U *a continuous symmetric tensor representation* $\mathcal{T}$;

(iv) g_0 *is a continuous positive definite reference tensor on* U;

(v) there exists $\alpha \in \mathbb{R}$ *such that*

$$g = g_0 + \alpha\mathcal{T} \tag{42}$$

is pointwise nondegenerate on U.

Then g *is a continuous metric-type tensor on* U.

Proof. The field g_0 is continuous, symmetric, and positive definite. The field $\mathcal{T}$ is continuous and symmetric by assumption. Hence g is continuous and symmetric. By nondegeneracy, $g(x)$ is invertible for every $x \in U$. Therefore g is a continuous nondegenerate symmetric $(0,2)$-tensor field on U. □

Remark 4.8. Theorem 4.7 is the proper mathematical form of the geometric conclusion. It does not assert that the entire variational model automatically produces a global metric. It does not assert Lorentzian signature. It states only that, when the local tensor representation exists and is nondegenerate relative to a reference tensor, the second-order response induces a continuous tensor of metric type.

Under additional regularity one may then recover the usual geometric machinery.

Corollary 4.9. *Under the hypotheses of Theorem 4.7, if $g \in C^1(U)$, then g determines a unique Levi–Civita connection on U. If $g \in C^2(U)$, then the associated Riemann curvature tensor is well defined.*

4.4 Interpretive summary

It is useful to isolate once more the exact logical chain proved or assumed up to this point. The model does not begin with a metric, nor does it conclude with one automatically. Instead, the analysis produces the following sequence:

$$\mathcal{A} \Longrightarrow \mathcal{J} \Longrightarrow \Phi_* \Longrightarrow \delta^2\mathcal{J}(\Phi_*) \Longrightarrow \mathcal{T} \Longrightarrow g. \tag{43}$$

The first four arrows are theorem-level statements under the standing hypotheses. The fifth is a representability hypothesis. The sixth is a nondegeneracy conclusion. The conceptual strength of the paper lies precisely in keeping those steps separate.

5 Discrete approximation and numerical illustrations

The continuum theory is variational and elliptic, so it admits a natural finite-difference realization in the quadratic case. The numerical part of the paper has a limited but important role. It does not replace analysis, and it does not serve as evidence for statements that have not been proved. Its purpose is twofold: first, to verify that the discrete solver reproduces the expected convergence behavior on a benchmark with known exact solution; second, to illustrate how the anchored minimizer and the reconstructed response tensor behave when the principal parameters of the model are varied.

5.1 Discrete quadratic action

To connect the continuum theory with computation, we discretize the quadratic model on a uniform Cartesian grid. The numerical scheme is designed to mirror, term by term, the same three-part structure that appears in the continuum action: discrete gradient energy, regularized anchor fidelity, and quadratic L^2-stabilization. We work on the unit square

$$\Omega = (0,1)^2 \tag{44}$$

with a uniform Cartesian grid of spacing

$$h = \frac{1}{m+1}. \tag{45}$$

Let $\Phi_{i,j}$ denote the discrete approximation of $\Phi(x_i, y_j)$ at the interior grid point $(x_i, y_j) = (ih, jh)$. Homogeneous Dirichlet conditions are imposed on the boundary.

The discrete counterpart of the quadratic action (13) is

$$\mathcal{J}_h(\Phi) = \frac{1}{2}\sum_{i,j}\left[\left(\frac{\Phi_{i+1,j}-\Phi_{i,j}}{h}\right)^2 + \left(\frac{\Phi_{i,j+1}-\Phi_{i,j}}{h}\right)^2\right]h^2 + \frac{\lambda}{2}\sum_{k=1}^{N}\left(\ell^h_{k,\varepsilon}(\Phi) - s_k\right)^2 + \frac{\mu}{2}\sum_{i,j}\Phi_{i,j}^2\,h^2. \tag{46}$$

The discrete anchor operator $\ell^h_{k,\varepsilon}$ is defined by Gaussian weights that approximate the continuum mollifier,

$$\ell^h_{k,\varepsilon}(\Phi) = \sum_{i,j}\omega^{(k)}_{i,j}\,\Phi_{i,j}, \qquad \omega^{(k)}_{i,j} = \frac{\exp\left(-\frac{|(x_i,y_j)-a_k|^2}{2\varepsilon^2}\right)}{\sum_{p,q}\exp\left(-\frac{|(x_p,y_q)-a_k|^2}{2\varepsilon^2}\right)}. \tag{47}$$

The normalization ensures

$$\sum_{i,j} \omega_{i,j}^{(k)} = 1. \tag{48}$$

Stationarity of $\mathcal{J}_h$ leads to the discrete Euler equation

$$-\Delta_h \Phi_{i,j} + \mu \Phi_{i,j} + \lambda \sum_{k=1}^{N} \Big(\ell_{k,\varepsilon}^{h}(\Phi) - s_k \Big) \omega_{i,j}^{(k)} = 0, \tag{49}$$

where Δ_h is the standard five-point Laplacian,

$$(\Delta_h \Phi)_{i,j} = \frac{\Phi_{i+1,j} + \Phi_{i-1,j} + \Phi_{i,j+1} + \Phi_{i,j-1} - 4\Phi_{i,j}}{h^2}. \tag{50}$$

This is the standard second-order finite-difference realization of the Laplacian on a Cartesian grid.

5.2 Manufactured-solution validation

The finite-difference scheme must first be validated on a problem with known exact solution. This is especially important here because the later tensor reconstruction depends on second derivatives of the discrete field. A solver that merely produces visually reasonable fields is not sufficient; the second-order structure must also converge correctly. We therefore consider

$$\Phi_{\mathrm{ex}}(x, y) = \sin(\pi x) \sin(\pi y), \tag{51}$$

which satisfies homogeneous Dirichlet conditions. For the model problem

$$-\Delta \Phi + \mu \Phi = f \qquad \text{in } \Omega, \qquad \Phi = 0 \qquad \text{on } \partial\Omega, \tag{52}$$

the forcing term is

$$f(x, y) = \Big(2\pi^2 + \mu \Big) \sin(\pi x) \sin(\pi y). \tag{53}$$

The grid errors are measured in the discrete norms

$$E_2(h) = \left(h^2 \sum_{i,j} |\Phi_{i,j} - \Phi_{\mathrm{ex}}(x_i, y_j)|^2 \right)^{1/2}, \tag{54}$$

and

$$E_\infty(h) = \max_{i,j} |\Phi_{i,j} - \Phi_{\mathrm{ex}}(x_i, y_j)|. \tag{55}$$

The observed rate between two successive meshes is

$$r(h) = \frac{\log(E(h)/E(h/2))}{\log 2}. \tag{56}$$

The numerical table below is computed for $\mu = 0.1$ and shows uniform second-order decay, exactly as expected for the centered finite-difference discretization.

Table 2: Manufactured-solution convergence for the discrete elliptic solver.

m	h	$E_2(h)$	$r_2(h)$	$E_\infty(h)$	$r_\infty(h)$
15	0.0625	1.5288×10^{-3}	—	3.0577×10^{-3}	—
31	0.03125	3.8240×10^{-4}	2.002	7.6480×10^{-4}	2.002
63	0.015625	9.5568×10^{-5}	2.000	1.9114×10^{-4}	2.000
127	0.0078125	2.3890×10^{-5}	2.000	4.7780×10^{-5}	2.000

The validation displayed in Figure 2 has a precise mathematical purpose. The later reconstruction of the tensor proxy depends on second derivatives of the discrete field, so qualitative stability of the

field solver alone is not sufficient. The discretization must converge at the level required to support a meaningful Hessian-based post-processing. The observed log–log decay therefore functions as a consistency check for the whole numerical stage of the paper, not merely for the field variable itself.

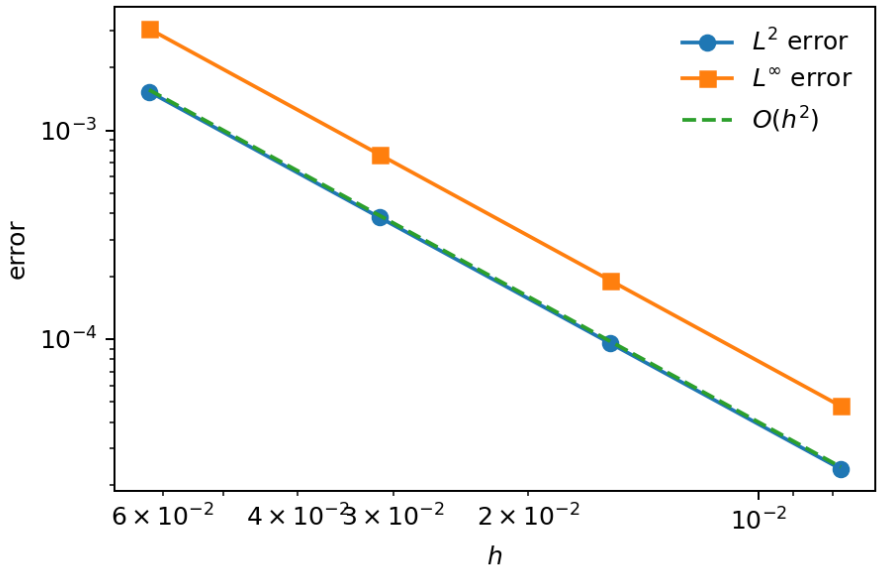

Figure 2: Manufactured-solution convergence for the finite-difference discretization of $-\Delta\Phi + \mu\Phi = f$. The log–log decay of both L^2- and L^∞-errors confirms second-order accuracy.

5.3 Anchor-driven field and tensor proxy

For the anchored computation we take three anchors,

$$\begin{aligned} a_1 &= (0.25, 0.25), \quad s_1 = 1.0, \\ a_2 &= (0.75, 0.35), \quad s_2 = -0.8, \\ a_3 &= (0.55, 0.80), \quad s_3 = 0.6. \end{aligned} \tag{57}$$

with equal weights $w_k = 1$, anchor width $\varepsilon = 0.03$, and parameters $\lambda = 1200$, $\mu = 0.1$.

The field profile shown in Figure 3 can be anticipated directly from the variational structure. The Dirichlet term suppresses oscillation, the anchor term drives the field toward the prescribed local averages, and the μ-term damps large global amplitudes. One therefore expects the minimizer to exhibit smooth localized rises and depressions centered near the anchors rather than singular spikes or uncontrolled oscillations. The computed surface confirms exactly this balance between regularity and anchor fidelity.

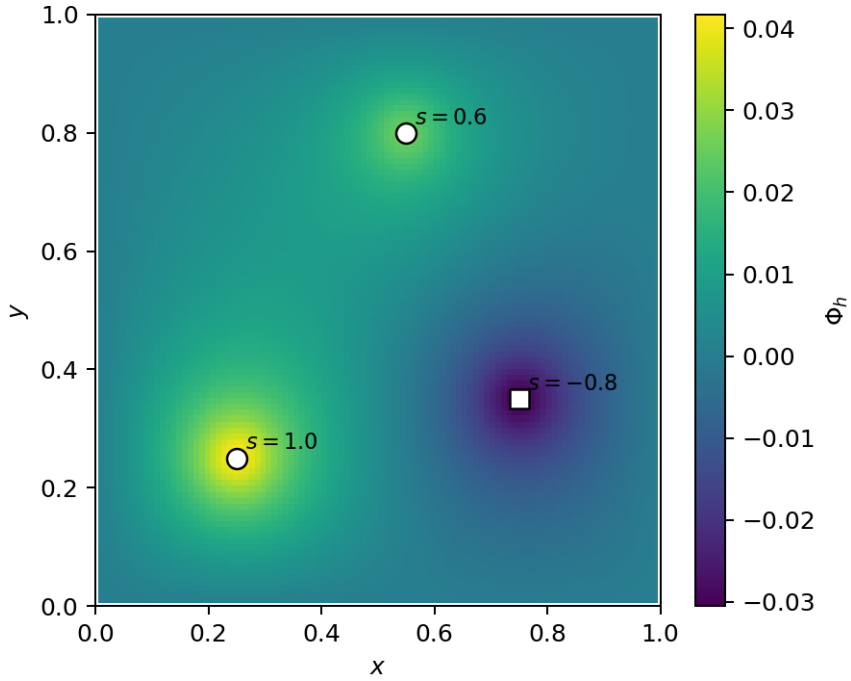

Figure 3: Discrete anchored minimizer Φ_h on $(0,1)^2$ for the three-anchor configuration (57). Positive anchors create elevated localized regions, while the negative anchor produces a smooth depression.

To reconstruct a positive-semidefinite tensor proxy, we approximate the second derivatives by centered differences. The purpose of this construction is not to assert that the raw discrete Hessian is itself the geometric tensor of interest. Rather, it is to build a discrete second-order quantity whose symmetry and positivity reflect the positivity of the continuum response form:

$$(\partial^h_{xx}\Phi)_{i,j} = \frac{\Phi_{i+1,j} - 2\Phi_{i,j} + \Phi_{i-1,j}}{h^2}, \tag{58}$$

$$(\partial^h_{yy}\Phi)_{i,j} = \frac{\Phi_{i,j+1} - 2\Phi_{i,j} + \Phi_{i,j-1}}{h^2}, \tag{59}$$

$$(\partial^h_{xy}\Phi)_{i,j} = \frac{\Phi_{i+1,j+1} - \Phi_{i+1,j-1} - \Phi_{i-1,j+1} + \Phi_{i-1,j-1}}{4h^2}. \tag{60}$$

The discrete Hessian is

$$H_h(\Phi)_{i,j} = \begin{pmatrix} (\partial^h_{xx}\Phi)_{i,j} & (\partial^h_{xy}\Phi)_{i,j} \\ (\partial^h_{xy}\Phi)_{i,j} & (\partial^h_{yy}\Phi)_{i,j} \end{pmatrix}, \tag{61}$$

and the tensor proxy is defined by

$$T_h = H_h(\Phi_h)^{\mathsf{T}} H_h(\Phi_h). \tag{62}$$

The corresponding discrete metric-type tensor is

$$g_h = I + \alpha T_h, \qquad \alpha > 0. \tag{63}$$

Because T_h is positive semidefinite at every grid point, g_h is pointwise positive definite for every $\alpha > 0$.

Two scalar diagnostics are used repeatedly:

$$M_h = \max_{i,j} \lambda_{\max}\Big(T_h(i,j)\Big), \tag{64}$$

and

$$R_h = \left\| -\Delta_h\Phi_h + \mu\Phi_h + \lambda \sum_{k=1}^{N} (\ell^h_{k,\varepsilon}(\Phi_h) - s_k)\omega^{(k)} \right\|_{\ell^2_h}. \tag{65}$$

5.4 Parameter sensitivity

The two most informative parameters are λ and ε. Increasing λ strengthens the penalty on anchor mismatch and should therefore amplify local curvature near the anchor locations. Increasing ε widens the coherence region and should therefore spread the response over a larger area, reducing peak curvature. The numerical results follow exactly this pattern.

The curve plotted in Figure 4 measures the maximal eigenvalue of the reconstructed tensor proxy T_h, not the amplitude of the field itself. It therefore tracks the intensity of the *second-order response* rather than the size of Φ_h. Its increase with λ shows that stronger anchor fidelity acts chiefly by sharpening the local curvature generated near the anchor set.

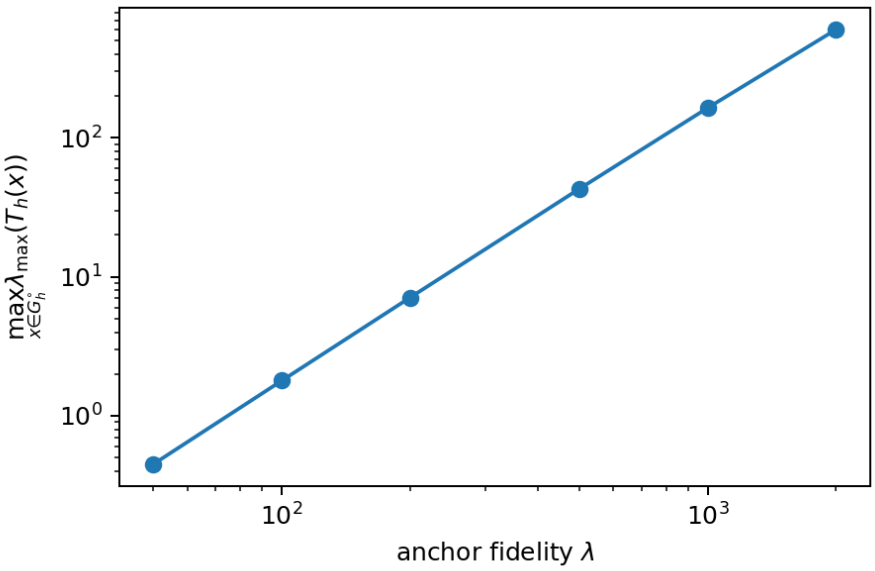

Figure 4: Dependence of the peak tensor-response amplitude M_h on the anchor-fidelity parameter λ, with $\varepsilon = 0.03$ and $\mu = 0.1$ fixed. Stronger anchor fidelity produces larger local curvature and hence a larger peak eigenvalue of T_h.

The complementary effect is shown in Figure 5. Enlarging ε does not remove anchor information; it redistributes that information over a wider averaging region. One therefore expects the discrete field to become smoother at grid scale and the tensor proxy to lose peak concentration. The monotone decrease of the plotted response is the numerical expression of that smoothing mechanism.

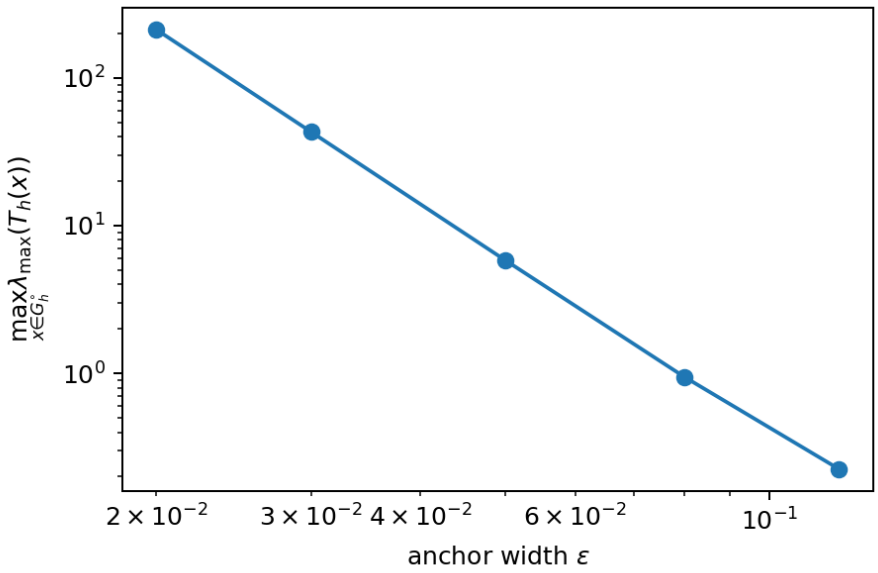

Figure 5: Dependence of the peak tensor-response amplitude M_h on the anchor width ε, with $\lambda = 500$ and $\mu = 0.1$ fixed. Wider anchor kernels spread the data constraint over a larger region and reduce the peak response of T_h.

The numerical evidence should be interpreted at the correct level. The computations do not establish a global geometric theorem. What they do establish is narrower and more relevant to the present paper: the discrete scheme is stable, the manufactured benchmark converges at the correct rate, and the tensor proxy reacts coherently to the model parameters in a way consistent with the continuum analysis.

6 Discussion and scope

The mathematical content of the paper is best read as a layered statement, with each layer resting on the previous one. The first layer concerns formulation. Once singular point evaluation is replaced by the mollified operators $\ell_{i,\varepsilon}$, the anchored action (10) becomes a legitimate functional on a Sobolev admissible class. The second layer concerns well-posedness: under the usual coercivity and weak lower-semicontinuity assumptions, the action admits minimizers. The third layer concerns structure: minimizers satisfy the weak Euler–Lagrange equation, and in the quadratic case they solve a linear elliptic equation with smooth localized forcing. The fourth layer concerns response: the second variation defines a symmetric bilinear form that is positive semidefinite under convexity assumptions. Only after these four layers are in place does the geometric question properly arise.

Read in this way, the paper does not ask the reader to accept a philosophical slogan. It asks the reader to follow a chain of precise mathematical implications. Each stage has its own input hypotheses, its own output statement, and its own level of interpretive force. The advantage of this layered presentation is that it makes visible exactly where proof ends and where additional hypotheses enter.

This order matters. It prevents the language of induced geometry from outrunning the variational analysis that is supposed to support it. In the present manuscript, the tensorial interpretation is attached to the second-order response, not to the scalar field itself. The scalar field Φ is an auxiliary variational quantity defined on a reference domain. The object with geometric significance is the response form $\delta^2\mathcal{J}$, and even then only after a local representability hypothesis has been imposed. This insistence on logical order is not merely expository discipline. It is part of the mathematical claim.

The Euclidean character of the framework should also be understood correctly. The domain $\Omega \subset \mathbb{R}^d$ and the elliptic operator $-\Delta + \mu$ provide a reference analytic stage on which gradients, weak convergence, mollifiers, and numerical discretizations can be defined cleanly. The resulting metric-type tensor, when it exists, is derived from the second-order response relative to that stage. Thus the present notion of emergence is restricted but precise: the metric-type object is not assumed in

the variational data, even though the analysis is carried out on a Euclidean background. For a first rigorous treatment, this restriction is a strength rather than a defect.

The same restraint applies to the numerical section. The manufactured-solution test confirms that the discrete elliptic solver and the Hessian-based tensor reconstruction exhibit the expected second-order behavior on smooth benchmark data. The anchor-driven experiments then show that the discrete minimizer and the tensor proxy respond coherently to variation of λ and ε. These computations support the internal consistency of the discrete realization, but they are not used as substitutes for proof. In particular, the choice $T_h = H_h^\top H_h$ is made because it preserves symmetry and positivity in the discrete setting and therefore reflects the continuum response form in a controlled way.

Several mathematical questions remain open. One concerns the singular limit $\varepsilon \to 0$. At the formal level, one expects the anchor functionals to approach point probes. At the analytic level, however, the Sobolev continuity that underlies the present existence proof becomes delicate, and a separate theory would be required. A second question concerns signature. The present response form is positive semidefinite under convexity assumptions and is naturally adapted to a Euclidean theory. Any passage to an indefinite or Lorentzian response would require a genuinely different mechanism. A third question concerns inverse design: given a prescribed response pattern, can one reconstruct or optimize an anchor configuration that realizes it? Each of these directions is mathematically natural, but each belongs to work beyond the scope of the present paper.

7 Conclusion

A regularized anchored variational model has been constructed and analyzed in a Sobolev framework. The decisive analytic idea is the replacement of singular point constraints by mollified anchor operators. With that replacement in place, the action admits the usual variational treatment: it is well defined on the admissible class, it possesses minimizers under standard hypotheses, and its minimizers satisfy a weak Euler–Lagrange equation. In the quadratic case, the field equation becomes a linear elliptic problem with smooth localized forcing and therefore fits naturally into classical regularity theory.

The second-order structure of the action is the central object of the paper. The second variation defines a symmetric response form and is positive semidefinite under convexity assumptions on the regularization. This response form is the only mathematically legitimate source of geometric interpretation in the present framework. When it admits a local tensor representation and satisfies a nondegeneracy condition relative to a positive definite reference tensor, it induces a continuous metric-type tensor. That statement is conditional, but it is also precise, and precision at this point is more important than breadth.

The resulting picture is therefore exact. A finite family of discrete localized anchors determines an anchored action. The anchored action determines a minimizing scalar field. The minimizing field determines a second-order response form. Under additional local hypotheses, that response form determines a tensor of metric type. This does not yet amount to a complete theory of emergent spacetime. It does, however, provide a rigorous variational foundation on which such questions can be posed without ambiguity.

For a reviewer, this is the principal mathematical message of the manuscript. The contribution is not that every aspect of geometry has been recovered from first principles. The contribution is that a carefully regularized anchored variational problem has been brought to the point where that larger question can be studied on a genuinely rigorous foundation.

A Expanded variational proofs

This appendix records the main variational arguments in expanded form. Nothing essentially new is proved here. The purpose is instead to remove any compression from the calculations and to make each passage between definitions, estimates, and weak limits completely explicit.

A.1 Continuity of the anchor operators

The estimate in Proposition 2.1 may be written more concretely as

$$|\ell_{i,\varepsilon}(\Phi)| = \left| \int_\Omega \rho_\varepsilon(x - a_i)\, \Phi(x)\, \mathrm{d}x \right| \le \left\| \rho_\varepsilon(\cdot - a_i) \right\|_{L^2(\Omega)} \|\Phi\|_{L^2(\Omega)}. \tag{66}$$

Since $H^1(\Omega) \hookrightarrow L^2(\Omega)$ continuously, there exists a constant $C_\Omega > 0$ such that

$$\|\Phi\|_{L^2(\Omega)} \le C_\Omega \|\Phi\|_{H^1(\Omega)}. \tag{67}$$

Combining (66) and (67) gives

$$|\ell_{i,\varepsilon}(\Phi)| \le C_\Omega \left\| \rho_\varepsilon(\cdot - a_i) \right\|_{L^2(\Omega)} \|\Phi\|_{H^1(\Omega)}. \tag{68}$$

Thus each anchor functional is bounded on $H^1(\Omega)$. In particular, if $\Phi_n \rightharpoonup \Phi$ weakly in $H^1(\Omega)$, then

$$\ell_{i,\varepsilon}(\Phi_n) \to \ell_{i,\varepsilon}(\Phi) \qquad \text{for each } i = 1, \dots, N. \tag{69}$$

This is the precise reason the anchored term behaves correctly under weak limits.

A.2 Existence by the direct method

We now prove Theorem 4.2 in detail. Let

$$m = \inf_{\Phi \in \mathcal{V}} \mathcal{J}(\Phi). \tag{70}$$

Choose a minimizing sequence $\{\Phi_n\} \subset \mathcal{V}$ satisfying

$$\mathcal{J}(\Phi_n) \downarrow m. \tag{71}$$

By coercivity, $\{\Phi_n\}$ is bounded in $H^1(\Omega)$. Since $H^1(\Omega)$ is reflexive, after passing to a subsequence there exists $\Phi_* \in H^1(\Omega)$ such that

$$\Phi_n \rightharpoonup \Phi_* \qquad \text{weakly in } H^1(\Omega). \tag{72}$$

Because $\mathcal{V}$ is closed and convex, it is weakly closed in the ambient Hilbert space; hence $\Phi_* \in \mathcal{V}$.

We pass to the limit term by term. Weak lower semicontinuity of the Dirichlet energy gives

$$\int_\Omega |\nabla \Phi_*|^2 \, \mathrm{d}x \le \liminf_{n\to\infty} \int_\Omega |\nabla \Phi_n|^2 \, \mathrm{d}x. \tag{73}$$

By (69),

$$\ell_{i,\varepsilon}(\Phi_n) \to \ell_{i,\varepsilon}(\Phi_*) \qquad \text{for each } i, \tag{74}$$

and therefore

$$\sum_{i=1}^N w_i \Big(\ell_{i,\varepsilon}(\Phi_*) - s_i \Big)^2 = \lim_{n\to\infty} \sum_{i=1}^N w_i \Big(\ell_{i,\varepsilon}(\Phi_n) - s_i \Big)^2. \tag{75}$$

Finally, weak lower semicontinuity of $\mathcal{R}$ gives

$$\mathcal{R}(\Phi_*) \le \liminf_{n\to\infty} \mathcal{R}(\Phi_n). \tag{76}$$

Combining (73), (75), and (76), we obtain

$$\mathcal{J}(\Phi_*) \le \liminf_{n\to\infty} \mathcal{J}(\Phi_n) = m. \tag{77}$$

Since $m \le \mathcal{J}(\Phi_*)$ by definition of the infimum, it follows that $\mathcal{J}(\Phi_*) = m$. Hence Φ_* is a minimizer.

A.3 Derivation of the first variation

Let $\Phi, \psi \in \mathcal{V}$. Consider the scalar function

$$F(t) = \mathcal{J}(\Phi + t\psi). \tag{78}$$

Differentiating the Dirichlet term gives

$$\frac{\mathrm{d}}{\mathrm{d}t}\Big|_{t=0} \frac{1}{2} \int_\Omega |\nabla(\Phi + t\psi)|^2 \, \mathrm{d}x = \int_\Omega \nabla\Phi \cdot \nabla\psi \, \mathrm{d}x. \tag{79}$$

Since $\ell_{i,\varepsilon}$ is linear,

$$\ell_{i,\varepsilon}(\Phi + t\psi) = \ell_{i,\varepsilon}(\Phi) + t\, \ell_{i,\varepsilon}(\psi), \tag{80}$$

and therefore

$$\frac{\mathrm{d}}{\mathrm{d}t}\Big|_{t=0} \frac{\lambda}{2} \sum_{i=1}^N w_i \Big(\ell_{i,\varepsilon}(\Phi + t\psi) - s_i\Big)^2 = \lambda \sum_{i=1}^N w_i \Big(\ell_{i,\varepsilon}(\Phi) - s_i\Big)\ell_{i,\varepsilon}(\psi). \tag{81}$$

The derivative of the regularization term is $\mu\, \delta\mathcal{R}(\Phi)[\psi]$. Summing these contributions yields (20).

A.4 Second variation and positivity

Differentiating (20) with respect to the base point Φ in a direction $\eta \in \mathcal{V}$ gives

$$\delta^2\mathcal{J}(\Phi)[\psi, \eta] = \int_\Omega \nabla\psi \cdot \nabla\eta \, \mathrm{d}x + \lambda \sum_{i=1}^N w_i\, \ell_{i,\varepsilon}(\psi)\, \ell_{i,\varepsilon}(\eta) + \mu\, \delta^2\mathcal{R}(\Phi)[\psi, \eta]. \tag{82}$$

The symmetry is immediate. Taking $\eta = \psi$ gives

$$\delta^2\mathcal{J}(\Phi)[\psi, \psi] = \big\|\nabla\psi\big\|^2_{L^2(\Omega)} + \lambda \sum_{i=1}^N w_i \Big(\ell_{i,\varepsilon}(\psi)\Big)^2 + \mu\, \delta^2\mathcal{R}(\Phi)[\psi, \psi]. \tag{83}$$

If $\mathcal{R}$ is convex, then $\delta^2\mathcal{R}(\Phi)[\psi, \psi] \geq 0$, and (83) is nonnegative.

A.5 Strong form in the quadratic case

In the quadratic case, the weak Euler–Lagrange identity (23) reads

$$\int_\Omega \nabla\Phi_* \cdot \nabla\psi \, \mathrm{d}x + \mu \int_\Omega \Phi_*\psi \, \mathrm{d}x + \lambda \sum_{i=1}^N w_i \Big(\ell_{i,\varepsilon}(\Phi_*) - s_i\Big) \int_\Omega \rho_\varepsilon(x - a_i)\psi(x) \, \mathrm{d}x = 0. \tag{84}$$

Using integration by parts on the gradient term, one obtains

$$-\Delta\Phi_* + \mu\Phi_* + \lambda \sum_{i=1}^N w_i \Big(\ell_{i,\varepsilon}(\Phi_*) - s_i\Big)\rho_\varepsilon(\cdot - a_i) = 0 \tag{85}$$

in the sense of distributions. This is the precise strong-form counterpart of the weak variational equation.

References

[1] J. M. Lee, *Introduction to Riemannian Manifolds*, 2nd ed., Graduate Texts in Mathematics, vol. 176, Springer, Cham, 2018. doi:10.1007/978-3-319-91755-9.

[2] S.-i. Amari, *Information Geometry and Its Applications*, Applied Mathematical Sciences, vol. 194, Springer, Tokyo, 2016. doi:10.1007/978-4-431-55978-8.

[3] M. Van Raamsdonk, Building up spacetime with quantum entanglement, *General Relativity and Gravitation* **42** (2010), no. 10, 2323–2329. doi:10.1007/s10714-010-1034-0.

[4] B. Swingle, Entanglement renormalization and holography, *Physical Review D* **86** (2012), no. 6, 065007. doi:10.1103/PhysRevD.86.065007.

[5] H. Brezis, A. Seeger, J. Van Schaftingen, and P.-L. Yung, Sobolev spaces revisited, *Atti della Accademia Nazionale dei Lincei, Classe di Scienze Fisiche, Matematiche e Naturali, Rendiconti Lincei Matematica e Applicazioni* **33** (2022), no. 2, 413–437. doi:10.4171/RLM/976.

[6] R. A. Adams and J. J. F. Fournier, *Sobolev Spaces*, 2nd ed., Pure and Applied Mathematics, vol. 140, Elsevier/Academic Press, Amsterdam, 2003.

[7] G. Leoni, *A First Course in Fractional Sobolev Spaces*, Graduate Studies in Mathematics, vol. 229, American Mathematical Society, Providence, RI, 2023. Also available at arXiv:2303.05940.

[8] B. Dacorogna, *Direct Methods in the Calculus of Variations*, 2nd ed., Applied Mathematical Sciences, vol. 78, Springer, New York, 2008. doi:10.1007/978-0-387-55249-1.

[9] I. Ekeland and R. Temam, *Convex Analysis and Variational Problems*, Classics in Applied Mathematics, vol. 28, Society for Industrial and Applied Mathematics, Philadelphia, PA, 1999. doi:10.1137/1.9781611971088.

[10] L. C. Evans, *Partial Differential Equations*, 2nd ed., Graduate Studies in Mathematics, vol. 19, American Mathematical Society, Providence, RI, 2010. doi:10.1090/gsm/019.

[11] D. Gilbarg and N. S. Trudinger, *Elliptic Partial Differential Equations of Second Order*, Classics in Mathematics, Springer, Berlin, 2001. doi:10.1007/978-3-642-61798-0.

[12] P. Grisvard, *Elliptic Problems in Nonsmooth Domains*, Classics in Applied Mathematics, vol. 69, Society for Industrial and Applied Mathematics, Philadelphia, PA, 2011. doi:10.1137/1.9781611972030.

[13] J. C. Strikwerda, *Finite Difference Schemes and Partial Differential Equations*, 2nd ed., Society for Industrial and Applied Mathematics, Philadelphia, PA, 2004. doi:10.1137/1.9780898717938.